Journal of Hazardous Materials 213–214 (2012) 318–324

Contents lists available at SciVerse ScienceDirect

Journal of Hazardous Materials

journal homepage: www.elsevier.com/locate/jhazmat

Evolution of natural organic matter by size exclusion chromatography during photocatalytic degradation by solvothermal-synthesized titanium dioxide

Sergio H. Valencia*, Juan M. Marín, Gloria M. Restrepo

Grupo Procesos Fisicoquímicos Aplicados, Universidad de Antioquia, Sede de Investigación Universitaria, cra. 53 # 61-30 Medellín, Colombia

ARTICLE INFO

Article history:
Received 5 December 2011
Received in revised form 27 January 2012
Accepted 1 February 2012
Available online 14 February 2012

Keywords:
Natural organic matter
Heterogeneous photocatalysis
Titanium dioxide
Solvothermal
Size exclusion chromatography

ABSTRACT

This study shows the effect of different titanium dioxides in transforming the structural properties of natural organic matter (NOM) during photocatalytic degradation with a solar UV light simulator. Titanium dioxide (TiO_2) synthesized by the sol–gel method coupled with the solvothermal technique and Degussa P-25 TiO_2 were used. The evolution of NOM degradation was followed by size exclusion chromatography with dissolved organic carbon, ultraviolet and fluorescence detection (SEC-DOC, SEC-UV_{254} and SEC-$Fl_{254/450}$). For both catalysts, there was a preferential degradation of the larger molecules of NOM into medium and smaller molecular size fractions. However, the synthesized TiO_2 was found to be more efficient than Degussa P-25 TiO_2 for DOC removal, especially UV_{254} absorption and $Fl_{254/450}$ removal.

1. Introduction

Natural organic matter (NOM) is formed from the decomposition of plant and animal residues [1]. It is an extraordinarily complex mixture of heterogeneous organic compounds, such as humic and fulvic acids [2]. The physico-chemical properties of NOM vary widely, depending on its source, age, fate and seasons of the years [3]. A supramolecular model was suggested which shows humic substances as composed of small and heterogeneous natural products held together by weak hydrophobic forces, van der Waals and H-bonds in only apparently large molecular sizes. Unlike macropolymers view stabilized by covalent bonds [4], the humic supramolecular structures chemical differences in humic matter rather to specific structural diversities [5,6].

NOM is the main precursor for the formation of hazardous disinfection byproducts (DBPs) upon reaction with chlorine or ozone in the water disinfection process. Trihalomethanes (THMs) and haloacetic acids (HAAs) are the most common DBPs in drinking waters [7], which are well-known to be mutagenic and carcinogenic halogenated compounds [8,9]. As such, it is critical to understand of NOM in established and possibly alternative water treatment steps.

Heterogeneous photocatalysis has widely been reported to effectively remove most organic pollutants. Among the various semiconductors, titanium dioxide (TiO_2) has been widely used [10]. There are several methods to synthesize TiO_2 nanoparticles, such as chemical vapor deposition [11], flame oxidation, sol–gel and solvothermal processes [12]. The solvothermal process leads to a fully anatase phase for the TiO_2 with nanocrystalline size and high surface area, lending itself to easy coating on different support materials [13].

Several published studies dealing with photocatalytic oxidation using Degussa P-25 TiO_2 showed it to be effective in the removal of NOM. However, most focused on the reduction of color, THMs, DOC and UV_{254} absorbance. These techniques are not adequate to fully understand the effect of photocatalytic treatment on NOM transformation, including evolution of the molecular size and changes in the nature of the NOM (e.g., UV_{254}, UV/vis absorption and fluorescence). In contrast, only a few studies have focused on the transformations occurring to the NOM during photocatalysis (e.g., Liu et al. [1] by high-performance size exclusion chromatography (SEC) with UV absorption detection (SEC-UV) and Tercero et al. [14] by size exclusion chromatography with DOC and UV_{254} absorbance detection (SEC-DOC/UV)).

This work therefore studied the evolution of molecular size distribution of the NOM of a bog lake during photocatalytic degradation with simulated solar UV irradiation by size exclusion chromatography with DOC, UV_{254} and fluorescence detection (SEC-DOC/UV_{254}/$Fl_{254/450}$), using TiO_2 synthesized by the sol–gel method, coupled with the solvothermal technique at low temperature (200 °C and 2 h) and the molar ratios (water/TIOT) = 3.5 and (2-propanol/TIOT = 15). The results were compared with Degussa P-25 TiO_2 under identical experimental conditions to study the influence of different properties of TiO_2 samples on NOM molecular size distribution.

* Corresponding author. Tel.: +57 4 2196543; fax: +57 4 2196543.
E-mail address: hvalens@gmail.com (S.H. Valencia).

0304-3894/$ – see front matter © 2012 Elsevier B.V. All rights reserved.
doi:10.1016/j.jhazmat.2012.02.003

2. Experimental

2.1. Materials and methods

Titanium dioxide (TiO_2, Degussa P-25), sodium hydroxide (0.1 N, Merck), hydrochloric acid (0.1 M, Merck), tetraisopropoxide titanium (TIOT) (98% purity, Merck) and 2-propanol (99.8%, Merck) were used as received from the supplier. NOM was taken from Lake Hohloh ("Hohlohsee", labeled HO-24), a bog lake in the Black Forest, Germany, which is extensively described elsewhere [15]. The lake water was filtered through 0.45 μm cellulose nitrate membrane filters (Merck) and stored in the dark at 4 °C. For the experiments, the filtered water was diluted to $\rho_0(DOC) = 10\ mg\ L^{-1}$ with ultrapure water (Milli-Q).

2.2. Synthesis of TiO_2 by the sol–gel method coupled with the solvothermal technique

Water and TIOT were slowly added to 2-propanol and stirred for 2 h at room temperature. Then, the gel was acidified with 0.0027 mol of HCl (3 mol L^{-1}). The molar ratios of water/TIOT and 2-propanol/TIOT were 3.5 and 15, respectively. TiO_2 synthesized with these molar ratios showed the highest anatase crystallinity and the highest NOM photodegradation. The mixture was next placed in a Teflon-lined stainless-steel reactor (autoclave) and heated at 200 °C for 2 h. The obtained precipitates were filtered using a 0.45 μm filter and washed with 30 mL of 2-propanol. The recovered material was dried at 80 °C for 1 h and ground to fine powder [13].

Synthesized TiO_2 was characterized using powder X-ray diffraction (XRD) by an X-ray diffractometer (Rigaku Miniflex) with Cu-Kα radiation in 2θ range from 10° to 60°. The reflectance diffusion spectrum UV–vis (UV/DRS) was obtained using an UV–vis Evolution 600 spectrometer, a thermo Electron Corporation with a reflectance diffuse accessory. Fourier transforms infrared (FTIR) spectroscopy by Prestige-21/FTIR-8400S spectrophotometer with an attenuated total reflectance (ATR) device. The superficial area of Brunauer–Emmett–Teller (BET) was determined using a Gemini V Miromerities V 2380 Instrument, with N_2 physisorption at 77 K, the sample was out degassed at 150 °C for 1 h in a Micromeritics Vac Preo 06 Kbars and purged using nitrogen for 2 h at 150 °C, prior to the surface area measurement [13].

2.3. Irradiation procedure

TiO_2 was suspended in 50 mL of filtered water at $\rho_0(DOC) \approx 10\ mg\ L^{-1}$. Up to nine samples, which were stirred and open to the atmosphere, were irradiated simultaneously from above by a homogeneous light field, using a solar UV simulator with an atmospheric attenuation filter (Oriel Corp., Stratford, USA) and additional WG 295 filters (6 mm, Shott Glaswerke, Mainz, Germany) installed in the radiation beam. The scheme and the details of the solar simulator are described elsewhere [16]. The radiation source was a 1000-W Xe short-arc lamp. The spectral irradiance was determined by spectral radiometry [17] in combination with polychromatic actinometry. The spectrum of the solar UV simulator contained relatively small portions of visible light compared to the real sunlight, while the cut-off wavelength in the UV range was situated nearly at the same wavelength as in real sunlight [16]. The estimated photon flow in the UV range ($290 < \lambda < 400$ nm) of the solar UV simulator was 1.4×10^{-7} mol s^{-1} (polychromatic actinometry following Defoin et al. [18]). The experimental temperature was maintained at 20 °C by a cooling circulator water bath. TiO_2 was immediately removed from the reaction medium by 0.4 μm HTTP membrane filters (Isopore, Millipore, Ireland) before analysis.

Table 1
Properties of synthesized TiO_2 by the sol–gel method coupled with the solvothermal technique (200 °C and 2 h), and Degussa P-25.

Property	Units	Synthesized TiO_2	Degussa P-25
Crystalline type	–	Anatase	Anatase (80%) Rutile (20%)
Crystallite size	Nm	6.71	30
BET	$m^2\ g^{-1}$	177.70	50
Bandgap indirect	eV	3.24	3.23

2.4. Dissolved organic carbon (DOC)

DOC concentrations were measured with a TOC-analyzer (TOC-V CSN 5050 Shimadzu, Japan). The samples were filtered through 0.45 μm polycarbonate membrane filters (Millipore, Ireland) prior to analysis.

2.5. UV/vis absorbance

The UV/vis absorbance in the range from $\lambda = 200$ to 750 nm was measured in a Cary 50 photometer (Varian Inc., USA) equipped with a quartz cell having a path length of 1 cm [19].

2.6. Size exclusion chromatography with organic carbon, ultraviolet and fluorescence detection (SEC-DOC, SEC-UV and SEC-Fl)

Size exclusion chromatograms of the filtered (0.45 μm) samples were obtained using a SEC-DOC/UV/Fl system developed by Huber and Frimmel [20] using Toyo-pearl HW 50S resin (Tosoh Corp., Japan) as column packing. This resin has a nominal molecular weight separation range from 100 g mol^{-1} to 18,000 g mol^{-1} (polyethylene glycols). The dimensions of the column were: length = 250 mm, inner diameter = 20 mm (Novogrom columns, Alltech Grom, Germany). Phosphate eluent (1.5 g L^{-1} $Na_2HPO_4{\cdot}2H_2O$ + 2.5 g L^{-1} KH_2PO_4) flowing at a rate of 1 mL min^{-1} as the mobile phase. Samples were diluted 1:5 prior to analysis. The injection volume was 1 mL and the DOC of each sample was calculated on the basis of an external calibration using potassium hydrogen phthalate as a standard. A photochemical oxidation of the sample components is carried out using a low-pressure mercury-vapor lamp (relevant emission wave lengths at 185 nm and 254 nm) in a special rotating thin-film reactor. Under these conditions, totally excluded molecules eluted after a retention time (t_r) of 28.7 min, while totally permeating molecules eluted after t_r of 66.3 min. A detailed description of the device and protocol was reported previously [19].

3. Results and discussion

3.1. Properties of TiO_2 synthesized

Table 1 shows the properties of the synthesized TiO_2 by the sol–gel method coupled with the solvothermal technique 200 °C and 2 h, with the molar ratios of water/TIOT = 3.5 and 2-propanol/TIOT = 15, and the properties of Degussa P-25 TiO_2. The synthesized TiO_2 presented differences in morphological and crystallographic properties compared with Degussa P-25 TiO_2. The DRX analysis showed that the synthesized TiO_2 had four characteristic peaks corresponding to the crystalline phase anatase ($2\theta = 25.3°$, 38.3°, 48.2° and 54.5°) and the peak corresponding to rutile phase was not observed ($2\theta = 27.46°$) [21] (Fig. not shown), whereas Degussa P-25 TiO_2 contains anatase and rutile phase in a ratio of about 3:1 [22]. The FTIR-ATR spectra show no

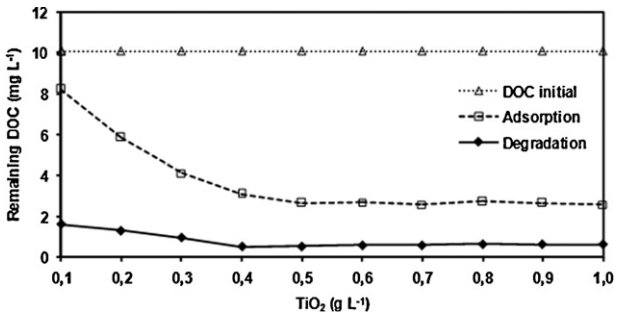

Fig. 1. Effect of synthesized TiO_2 dosage on NOM adsorption and photodegradation. ρ_0(DOC) = 10 mg L^{-1}, pH = 5.0, adsorption time = 60 min, photocatalytic degradation time = 180 min.

significant differences. The average particle size calculated by applying the Scherer formula [23] on the anatase diffraction peaks showed synthesized TiO_2 has small particle size, and BET analysis showed this method of synthesis leads to higher surface area compared to Degussa P-25 TiO_2. However, both catalysts presented similar indirect bandgap values for anatase, obtained using the Kubelka–Munk reemission function [24]. The literature reports an indirect band gap of 3.23 eV for anatase phase [25]. Detailed morphological characterization of synthesized TiO_2 by the sol–gel method coupled with the solvothermal technique has been reported elsewhere [13].

3.2. Photolysis and adsorption experiments in the dark

The simulated UV irradiation in the absence of the synthesized TiO_2 did not produce changes in DOC concentrations during 270 min of reaction. The adsorption equilibrium of NOM onto synthesized TiO_2 in the dark was reached in less than 5 min (data not shown). For all experiments that followed, an adsorption time of 60 min was chosen to ensure the equilibrium state.

3.3. Effect of synthesized TiO_2 dosage on the adsorption and removal of NOM

Fig. 1 shows the remaining DOC as a function of synthesized TiO_2 dosage after adsorption in the dark to reach equilibrium state, and after photocatalytic degradation. The amount of DOC adsorbed increased with increasing $\rho(TiO_2)$ up to 0.5 g L^{-1}. Any further addition of TiO_2 did not change the DOC adsorption. The DOC removal during photodegradation increased with increasing $\rho(TiO_2)$ between 0.1 and 0.4 g L^{-1} due to an increased number of active sites. At higher $\rho(TiO_2)$, the DOC removal remained constant because the turbidity of the suspension reduced the effective UV irradiation [26]. Therefore, the optimum $\rho(TiO_2)$ was 0.4 g L^{-1}. The DOC conversion at this $\rho(TiO_2)$ was 94.9% after 270 min of irradiation.

The Langmuir–Hinshelwood (L–H) model is commonly employed to quantitatively describe heterogeneous reactions [27]. For low liquid-phase concentrations of the organic substrate a pseudo-first-order reaction can be used, $\ln C_0/C_t = -k_a t$ [28], where k_a (min^{-1}) denotes the pseudo-first-order reaction rate constant and C_0 is the initial concentration of substrate or the specified UV–vis parameters. To determine the kinetic data for DOC and UV_{254} during the photodegradation with synthesized TiO_2, the relationship between $\ln C_0/C_t$ and irradiation time was plotted [29]. It was found that the photodegradation of NOM under the synthesized TiO_2 obeyed first-order reaction kinetics (Table 2). The k_a of UV_{254} removal is significantly higher than the k_a of DOC removal, implying that the loss of aromaticity and insaturation of the substances is easier achieved than their mineralization [30].

Table 2
Pseudo first-order kinetic (k_a, min^{-1}) parameters as a function of synthesized TiO_2 dosage over 270 min of irradiation time.

$\rho(TiO_2)$ (g L^{-1})	k_a DOC	R^2	k_a UV_{254}	R^2
0.2	0.009	0.900	0.016	0.941
0.4	0.012	0.904	0.018	0.937
0.6	0.011	0.923	0.017	0.921

3.4. Changes in molecular weight, UV_{254} and fluorescence by SEC-DOC, SEC-UV_{254} and SEC-$Fl_{254/450}$

Fig. 2 shows the SEC-DOC (a), SEC-UV_{254} (b), and SEC-$Fl_{254/450}$ (c) chromatograms of the NOM during the photocatalytic degradation of NOM with synthesized TiO_2, using the solar UV simulator (batch reactor), with $\rho_0(DOC) \approx 10$ mg L^{-1} at pH = 5.0 and $\rho(TiO_2) = 0.4$ g L^{-1}. UV_{254} is mainly absorbed by aromatic rings and conjugated double bonds [2], and the fluorescence at $\lambda_{ex} = 254$ nm and $\lambda_{em} = 450$ nm is typical for humic acids [31].

SEC chromatograms (Fig. 2) were divided into three fractions corresponding to the retention time (t_r) (numerically equal to the elution volume in mL in this case). These fractions were labeled F1–F3. F1 was defined in the interval 28.0 min < t_r < 45.8 min and attributed to humic material [32]. F2 was between 45.8 min < t_r < 50.7 min and contained aromatic and polyfunctional organic acids, but mainly aromatic organic acids [33,34]. F3 was defined between 50.7 min < t_r < 56.5 min and included totally permeating molecules, as well as molecules which elute prematurely due to the difference in electrical conductivity between sample and buffer [14,32,34].

The shape and distributions of size fractions of NOM in an SEC is sensitive to minor changes of solutions parameters [35]. The UV-detection of NOM during SEC may be negatively affected by the presence of high concentrations of UV-absorbing inorganic ions (e.g. nitrate, iron) or UV-scattering particles [36]. The original Lake Hohloh water contained $\ll 1$ μmol L^{-1} of each Cu and Mn, approx 2 μmol L^{-1} for Zn, and approx. 6 μmol L^{-1} for Fe, as measured by inductively coupled plasma optical emission spectroscopy (ICP-OES). This elemental analysis data indicate that the content of inorganic substances in the row water was low with reference to Weishaar et al. [37], who found significant UV absorbance values at 254 nm only above a concentration of 500 μg L^{-1} for Fe and 40 mg L^{-1} for nitrate. Therefore, UV-absorption resulting from the presence of inorganic chromophores is negligible, and UV-absorption is caused by the NOM.

SEC-DOC (Fig. 2a) shows a high adsorption of NOM onto synthesized TiO_2 in the dark with significant removal for all investigated fractions. There was not preferential adsorption for any NOM fraction. However, the larger fraction of NOM (F1) were preferentially degraded during the irradiation time, and F1 shifted continuously towards longer retention times (lower weight size). It implies that mineralization did not proceed directly to CO_2, but occurred by the breakdown of larger molecules into smaller size fractions. After 60 min of irradiation, there was near complete removal of F1 with concurrent increases in F2 and F3. Following 120 min of irradiation, a complete removal of F1 was reached with a nearly complete disappearance of F2, whereas F3 continued to grow. Following 180 min, F3 began to decline, whereas F2 was practically depleted, and after 240 min, F3 continued to decline.

The SEC-UV_{254} measurements (Fig. 2b) were qualitatively similar to those from SEC-DOC, but the transformations occurred faster. SEC-UV_{254} shows a high adsorption of NOM with high UV_{254} absorption onto synthesized TiO_2 in the dark. There was significant adsorption for all fractions studied. After 60 min of irradiation, there was a rapid reduction in F1 with concurrent increases in F2 and F3. Following 120 min of irradiation, F1 and F2 were completely

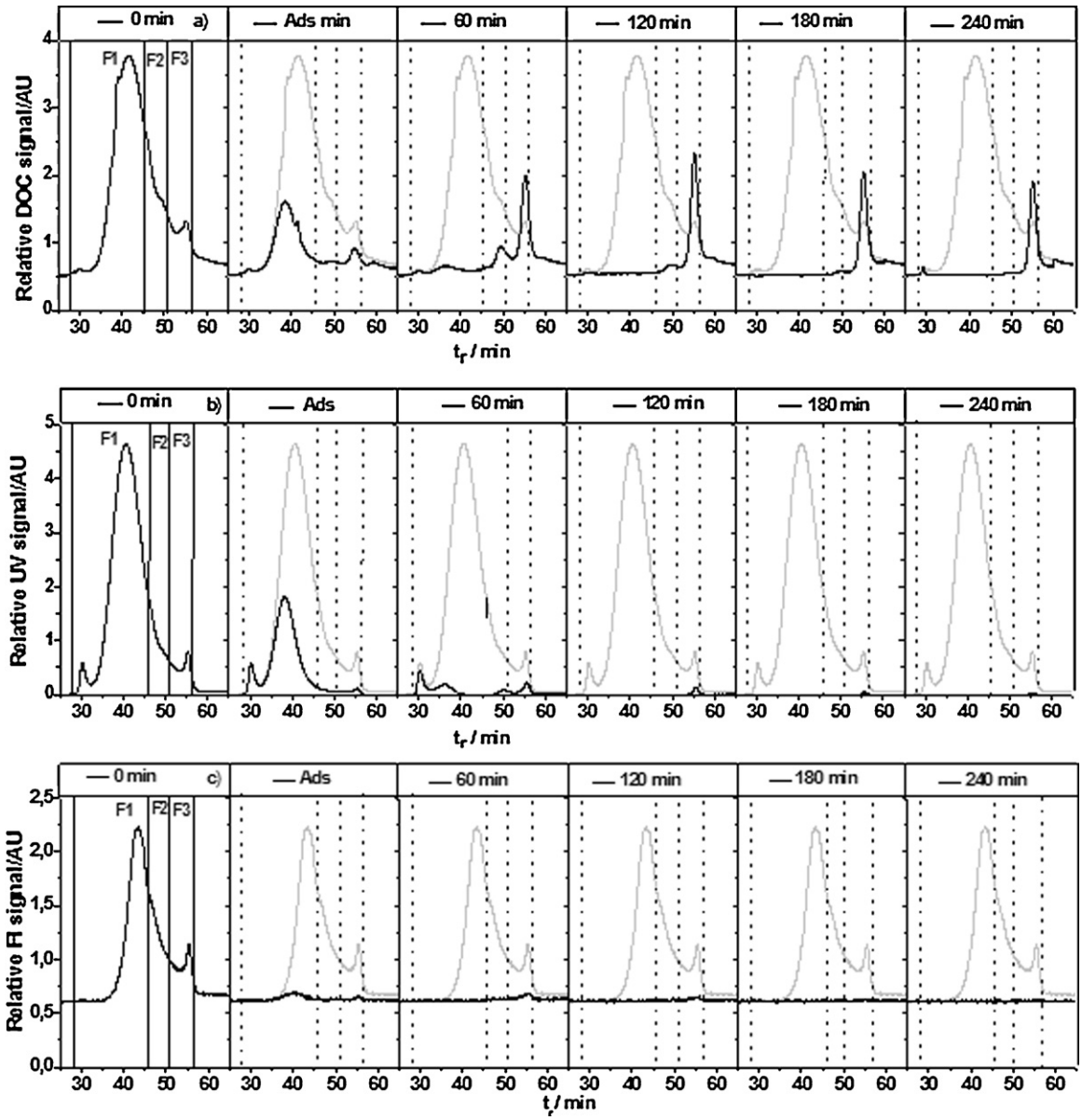

Fig. 2. SEC-DOC (a), SEC-UV_{254} (b) and SEC-$Fl_{254/450}$ (c) chromatograms of NOM showing fractions F1–F3 and their time evolution during photodegradation with synthesized TiO_2. $\rho(TiO_2) = 0.4\ g\ L^{-1}$ and pH = 5. Ads: adsorption, gray line is SEC chromatogram of NOM at $t = 0$ min (without adsorption and degradation).

removed, with a slight reduction in F3. Following 180 min of irradiation, there was no remaining significant UV absorption for the samples.

SEC-$Fl_{254/450}$ (Fig. 2c) shows near complete adsorption of fluorescents compounds, and the transformation occurred faster than in SEC-DOC and SEC-UV_{254}, such that at 60 min of irradiation there is not significant fluorescence intensity. Thus, phocatalysis with synthesized TiO_2 broke down the high molecules into smaller molecules with less intensity fluorescence.

Therefore, the photodegradation of NOM with synthesized TiO_2 demonstrated selectivity. The NOM photodegradation proceeded with a preferential degradation of larger molecules with high UV_{254} absorption and fluorescence intensity into smaller with lesser UV_{254} absorbance and fluorescence intensity. Tercero et al. [14] reported that the preferential photodegradation of the larger molecules of NOM was due to the preferential adsorption of these large molecules onto Degussa P-25 TiO_2 in the dark. However, the SEC chromatogram with synthesized TiO_2 showed no preferential adsorption of F1 in the dark, but it did show a preferential degradation of F1. To this end, the reaction between •OH and NOM depends on the molecular weight, where •OH reacted preferentially with higher molecular weight structures. They tend to be more aromatic and may have a larger number of available reactions [2]. Additionally, Westerhoff et al. [38] observed for different NOM isolates a positive correlation between the molecular weight and aromaticity of NOM and the reaction constant between •OH and the NOM. Neverthless, although •OH also attacks medium and small fractions (F2 and F3), their rate of formation exceeded their rate of degradation. Consequently, there was an overall increase in the concentration of F2 and F3 at the expense of F1.

3.5. Changes in UV/vis absorption of NOM with TiO_2 synthesized

A steady decrease in the UV/vis absorption of NOM was observed with increasing irradiation time from 60 to 180 min (Fig. 3). Following 180 min of irradiation, there was a small amount of organic matter, which persisted even after 240 min of irradiation, indicating that complete mineralization could not be achieved. This resistant

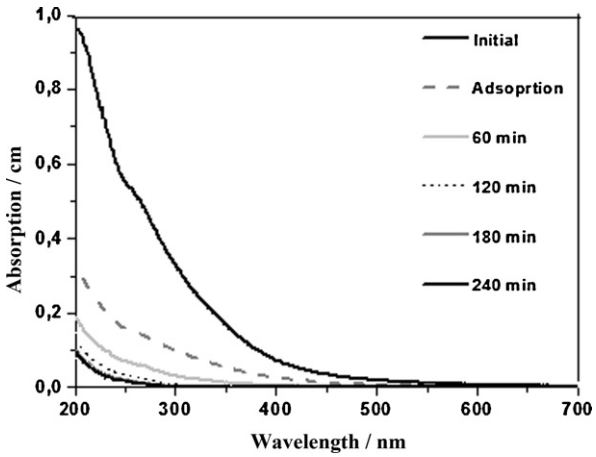

Fig. 3. Effect of irradiation time on UV/vis absorption spectral during photocatalytic degradation of NOM with synthesized TiO_2. $\rho_0(DOC) \approx 10\,mg\,L^{-1}$ at pH = 5 and $\rho(TiO_2) = 0.4\,g\,L^{-1}$.

fraction was composed of refractory compounds found in the original NOM solution or byproducts of partial oxidation [30].

Table 3 shows the specific absorbance parameters and spectroscopy ratios of NOM during photocatalytic degradation with synthesized TiO_2, using the solar UV simulator (batch reactor), with $\rho_0(DOC) \approx 10\,mg\,L^{-1}$ at pH = 5.0 and $\rho(TiO_2) = 0.4\,g\,L^{-1}$. The specific UV absorbance (SUVA, $L\,mg^{-1}\,m^{-1}$) is defined as the UV absorbance per milligram of organic carbon, and the specific color absorbance ($SCOA_{436}$, $L\,mg^{-1}\,m^{-1}$) is defined as $Color_{436}$ per milligram of organic carbon.

$SUVA_{254}$ represents the UV-absorbing aromatic structures and double bonds of NOM [2], and high $SUVA_{254}$ values indicates that the organic matter is composed largely of hydrophobic and high apparent molecular weight [39]. This parameter can be used to describe the composition of water in terms of hydrophobicity and hydrophilicity. An $SUVA_{254} > 4$ indicates mainly hydrophobic and especially aromatic material, whereas $2 < SUVA_{254} < 4$ represents a mixture of hydrophobic and hydrophilic NOM and $SUVA_{254} < 2$ represents hydrophilic material [40]. $SUVA_{365}$ has been demonstrated that increase with increasing molecular [41]. The absorbance value at $\lambda = 436$ nm ($Color_{436}$) represents the color-forming moieties, and it is used to estimate the content of quinones in HS samples [42].

All specific absorbance parameters (SUVA and $Color_{436}$) significantly decreased (Table 3), implying a reduction of aromatic compounds and double bonds, a decrease in molecular size, and the reduction of quinones. Moreover, the NOM composition changed from hydrophobic to hydrophilic after 120 min of irradiation ($SUVA_{254} < 2$). This residual organic matter with these properties is less reactive with chlorine to form disinfection by-product (DBPs) such as trihalomethanes (THMs) [3]. A strong linear correlation between DOC and $SUVA_{254}$, $SUVA_{365}$ and $SCOA_{436}$ was found, with the correlation coefficients (R^2) 0.976, 0.983 and 0.976, respectively.

Table 3
SUVA ($m^{-1}\,mg^{-1}\,L$) as a function of irradiation time in NOM photocatalytic degradation with synthesized TiO_2. $\rho_0(DOC) \approx 10.0\,mg\,L^{-1}$ at pH = 5 and $\rho(TiO_2) = 0.4\,g\,L^{-1}$.

Time (min)	DOC	$SUVA_{254}$	$SUVA_{365}$	$SCOA_{436}$
0	10.14	5.27	1.31	0.42
Ads	3.71	4.14	1.19	0.43
60	3.09	2.16	0.31	0.09
120	1.91	1.68	0.09	0.03
180	1.19	0.59	0.07	0.02
240	0.59	0.64	0.10	0.04
Removal (%)	94.1	87.7	92.3	89.6

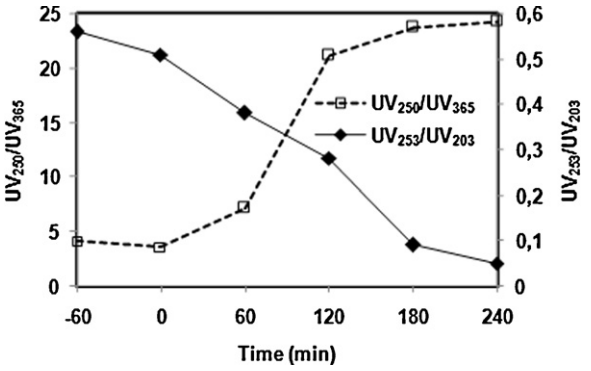

Fig. 4. E_{253}/E_{203} and E_{250}/E_{365} parameters during NOM photocatalytic degradation with synthesized TiO_2. $\rho_0(DOC) \approx 10\,mg\,L^{-1}$ at pH = 5 and $\rho(TiO_2) = 0.4\,g\,L^{-1}$.

Fig. 4 shows the ratios of the UV/vis absorption at 253–203 nm (E_{253}/E_{203}) and absorption at 250 nm to 365 nm (E_{250}/E_{365}) of NOM during photocatalytic degradation with synthesized TiO_2, using the solar UV simulator (batch reactor), with $\rho_0(DOC) \approx 10\,mg\,L^{-1}$ at pH = 5.0 and $\rho(TiO_2) = 0.4\,g\,L^{-1}$. The E_{253}/E_{203} is low for unsubstituted aromatic ring structures and increased for NOM with hydroxyl, carbonyl, ester and carboxylic functional groups [42]. These groups participate preferentially in reactions to generate DBPs [43]. The E_{250}/E_{365} has been reported to correlate with the molecular size and aromaticity, increasing as the aromaticity and the molecular size decrease [40]. As seen from the data, there was a gradual decrease in molecular size (E_{250}/E_{365} increased) and an increase in electrophilic structures and unsaturated bonds (E_{253}/E_{203} decreases) during the photocatalytic degradation of NOM. These results are consistent with SEC analysis.

3.6. Comparison of synthesized TiO_2 with Degussa P-25 TiO_2 in the photodegradaton of NOM

The effectiveness of synthesized TiO_2 in the photodegradation of NOM was compared with Degussa P-25 TiO_2 under identical experimental conditions except for using $\rho(TiO_2) = 0.6\,g\,L^{-1}$ of Degussa P-25. This amount was found to be optimal for Degussa P-25 (data not shown). Fig. 5 shows the resulting SEC-DOC (a), SEC-UV_{254} (b) and SEC-$Fl_{254/450}$ (c) chromatograms [44].

We found two differences in NOM photodegradation between Degussa P-25 and synthesized TiO_2. First, Degussa P-25 TiO_2 presented a preferential adsorption of the large fraction (F1) in the dark for DOC, UV_{254} and $Fl_{254/450}$ (Fig. 5), whereas synthesized TiO_2 presented a high adsorption for all fractions (F1–F3). However, the sequence of the photodegradation remained constant. For both catalysts, the growth of the smaller fractions (F2–F3) occurred at the expense of the large fraction (F1).

Second, the synthesized TiO_2 was more efficient than Degussa P-25 for the photocatalytic removal of DOC, especially the removal of UV_{254} absorption and $Fl_{250/450}$, implying higher loss of aromaticity and conjugated double bonds, which are associated with the main precursor for DBPs [45]. SEC-DOC with Degussa P-25 TiO_2 (Fig. 5a) shows a larger increase in DOC content for F2 and F3 after 60 min of irradiation in comparison to synthesized TiO_2 (Fig. 2a), although both catalysts showed only small differences in F1 removal, due to after 60 min of irradiation there was near complete removal of F1. Nevertheless, following 120 min and 240 min of irradiation, the rate of degradation of F3 was similar for both catalysts; implying complete mineralization could not be achieved. SEC-UV_{254} shows a clear effect of the catalyst on UV_{254} absorption removal. Degussa P-25 TiO_2 (Fig. 5b) presented a larger increase in UV_{254} absorption of F2 and F3 after 60 min of irradiation in comparison to the synthesized TiO_2 (Fig. 2b). SEC-$Fl_{254/450}$ shows that Degussa P-25 TiO_2

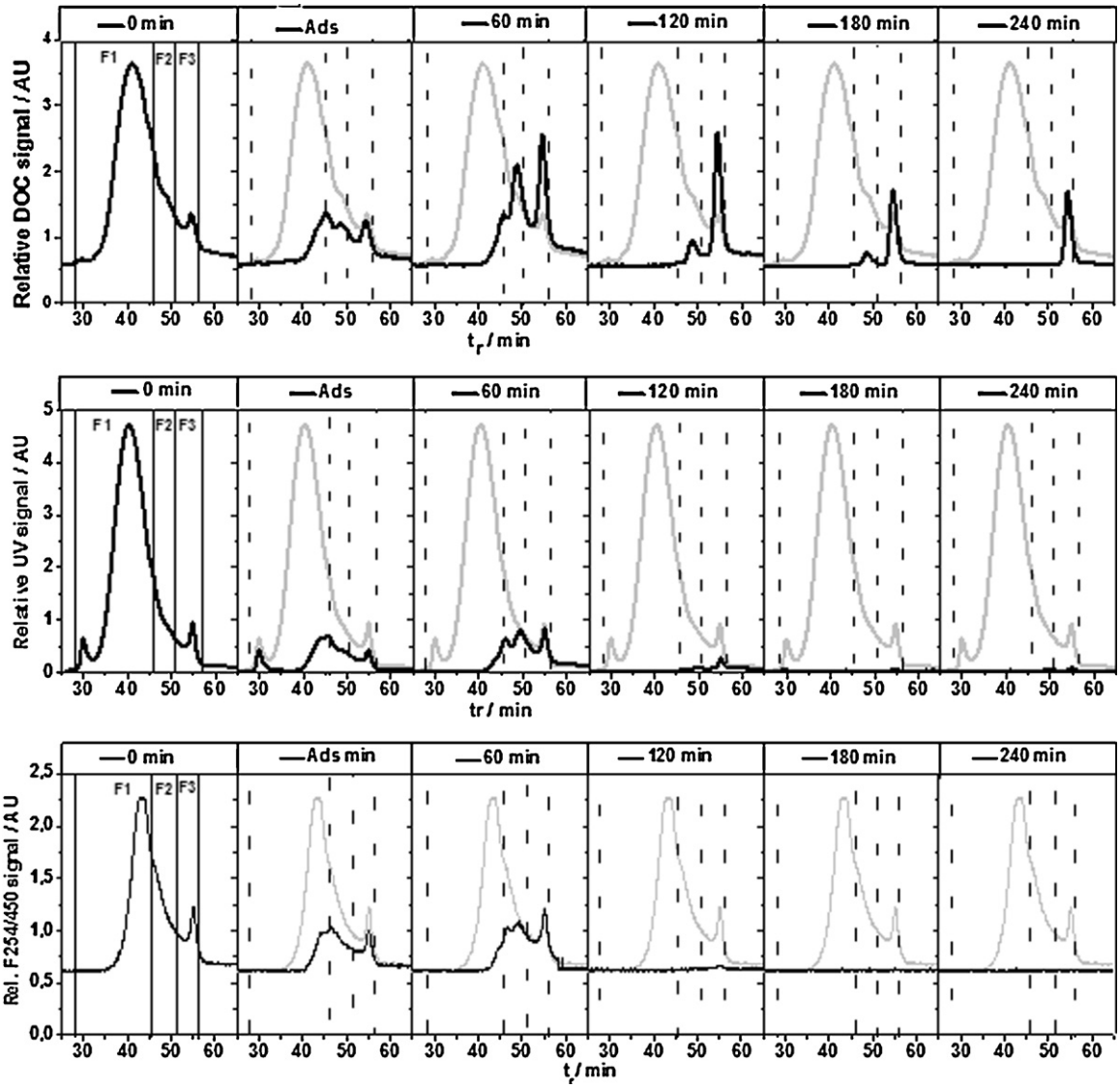

Fig. 5. SEC-DOC (a), SEC-UV_{254} chromatograms (b) and SEC-$Fl_{254/450}$ (c) of NOM showing the fractions F1–F3 and their time evolution during photodegradation with Degussa P-25 TiO_2. $\rho(TiO_2) = 0.6\ g\ L^{-1}$ and pH = 5. Ads: adsorption, gray line is SEC chromatogram of NOM at $t = 0$ min (without adsorption and degradation).

(Fig. 5b) presented an increase in $Fl_{254/450}$ of F2 and F3 after 60 min of irradiation, whereas synthesized TiO_2 lead to complete removal of all fractions (F1–F3). It shows there was retardation in the degradation of F2 and F3 fractions with Degussa P-25 TiO_2. Therefore, the photocatalytic process with the synthesized and Degussa P-25 TiO_2 proceed at different velocities and lead to different products and size distributions of the metabolites of the original NOM, although the sequence of the photodegradation remained constant for both catalysts.

The differences in morphological and crystallographic properties of synthesized and Degussa P-25 TiO_2, such as the specific surface, crystalline size and the crystalline phases (anatase or anatase-rutile) did not affect the selectivity for NOM photodegradation. Nevertheless, they did affect the efficiency of the photodegradation process. The reason for this was the differences in their NOM adsorption in the dark [46]. The synthesized TiO_2 had a higher capacity for NOM adsorption in the dark (63.4% and 47.5% of DOC for synthesized and Degussa P-25, respectively), and the synthesized TiO_2 did not present a preferential adsorption of the larger molecular weight fraction in the dark due to its high surface area. This emphasized the importance of the specific surface area in NOM photocatalytic degradation [47].

4. Conclusions

TiO_2 synthesized by the sol–gel method with the solvothermal technique in the molar ratios of water/TIOT = 3.5 and 2-propanol/TIOT = 15 showed higher efficiency than Degussa P-25 TiO_2 for the photocatalytic degradation of NOM. The results showed that the high adsorption of the NOM onto synthesized TiO_2 in the dark, due to its high specific surface area, led to a faster rate of NOM photodegradation. The differences in morphological and crystallographic properties of synthesized and Degussa P-25 TiO_2, such as the specific surface, crystalline size and the crystalline phases (anatase or anatase-rutile) did not affect the selectivity of photodegradation of NOM. For both catalysts, NOM was preferentially degraded into medium and smaller molecular size fractions. Subsequent degradation led to near complete removal of these molecular size fractions in the tested samples.

Acknowledgements

We are grateful to the Universidad de Antioquia (Colombia), Expedición Antioquia 2013 Program and Colciencias for financial support. We thank Professor F.H. Frimmel, and we are grateful to Matthias Weber for performing the size-exclusion chromatographic (SEC) analysis (Water Chemistry, Engler-Bunte-Institut, Universität Karlsruehe (TH), Germany).

References

[1] S. Liu, M. Lim, R. Fabris, C. Chow, M. Drikas, R. Amal, TiO_2 photocatalysis of natural organic matter in surface water: impact on trihalomethane and haloacetic acid formation potential, Environ. Sci. Technol. 42 (2008) 6218–6223.
[2] S. Sarathy, M. Mohseni, The impact of UV/H_2O_2 advanced oxidation on molecular size distribution of chromophoric natural organic matter, Environ. Sci. Technol. 41 (2007) 8315–8320.
[3] S. Liu, M. Lim, R. Fabris, C. Chow, M. Drikas, R. Amal, Comparison of photocatalytic degradation of natural organic matter in two Australian surface waters using multiple analytical techniques, Org. Geochem. 41 (2010) 124–129.
[4] K. Ghosh, M. Schnitzer, Macromolecular structure of humic substances, Soil Sci. 129 (1980) 266–276.
[5] P. Conte, R. Spaccini, D. Smejkalová, A. Nebbioso, A. Piccolo, Spectroscopic and conformational properties of size-fractions separated from a lignite humic acid, Chemosphere 69 (2007) 1032–1039.
[6] C. Maia, A. Piccolo, A. Mangrich, Molecular size distribution of compost-derived humates as a function of concentration and difference counterions, Chemosphere 73 (2008) 1162–1166.
[7] A. Matilainen, M. Sillanpää, Removal of natural organic matter from drinking water by advanced oxidation processes, Chemosphere 80 (2010) 351–365.
[8] P. Singer, DBPs in drinking water: additional scientific and policy considerations for public health protection, J. Am. Water Works Assoc. 98 (2006) 73–79.
[9] B. Eggins, F. Palmer, A. A. Byrne, Photocatalytic treatment of humic substances in drinking water, Water Res. 31 (1997) 1223–1226.
[10] S. Valencia, F. Catano, L. Rios, G. Restrepo, J. Marín, A new kinetic model for heterogeneous photocatalysis with titanium dioxide: case of non-specific adsorption considering back reaction, Appl. Catal. B: Environ. 104 (2011) 300–304.
[11] O. Carp, C. Huisman, A. Reller, Photoinduced reactivity of titanium dioxide, Progr. Solid State Chem. 32 (2004) 33–177.
[12] M. Kallala, C. Sanchez, B. Cabane, Structures of inorganic polymers in sol–gel processes based on titanium oxide, Phys. Rev. E 48 (1993) 3692–3704.
[13] S. Valencia, J. Marín, G. Restrepo, Study of the bandgap of synthesized titanium dioxide nanoparticules using the sol–gel method and a hydrothermal treatment, Open Mater. Sci. J. 4 (2010) 9–14.
[14] L.A. Tercero, E.T. Haseborg, M. Weber, F.H. Frimmel, Investigation of photocatalytic degradation of brown water natural organic matter by size exclusion chromatography, Appl. Catal. B: Environ. 87 (2009) 56–62.
[15] F.H. Frimmel, G. Abbt-Braun, K.G. Heumann, B. Hock, H.-D. Ludemann, M. Spiteller, Refractory Organic Substances (ROS) in the Environment, John Wiley and Sons, New York, 2002, pp. 281–304.
[16] T.E. Doll, F.H. Frimmel, Fate of pharmaceutical photodegradation by simulated solar UV light, Chemosphere 52 (2003) 1757–1769.
[17] A.J. Schindelin, Photochemisher Abbau Anthropogener Organischer Substanzen im Wasser Mittels Simulierter und Natürlicher Solarer Strahlung, Dissertation Universität, Karlsruhe, 1998.
[18] A. Defoin, R. Defoin-Stratmann, K. Hildenbrand, E. Bittersmann, D. Kreft, H.J. Kuhn, A new liquid phase actinometer: quantum yield and photo-CIDNP study of phenylglyoxylic acid in aqueous solutions, J. Photochem. 33 (1986) 237–255.
[19] T.E. Doll, F.H. Frimmel, Photocatalytic degradation of carbamazepine, clofibric acid and iomeprol with P25 and Hombikat UV100 in presence of natural organic matter (NOM) and other organic water constituents, Water Res. 39 (2005) 403–411.
[20] S.A. Huber, F.H. Frimmel, Flow injection analysis for organic and inorganic carbon in the low-ppb range, Anal. Chem. 63 (1991) 2122–2130.
[21] G. Liu, Z. Jin, T. Wang, Z. Liu, Anatase TiO_2 porous thin films prepared by sol–gel method using CTAB surfactant, J. Sol–Gel Sci. Technol. 41 (2007) 49–55.
[22] T. Ohno, K. Sarukawa, K. Tokieda, M. Matsumara, Morphology of a TiO_2 photocatalyst (Degussa, P-25) consisting of anatase and rutile crystalline phases, J. Catal. 1 (2001) 82–86.
[23] N. Venkatachalam, M. Palanichamy, V. Murugesan, Sol–gel preparation and characterization of nanosize TiO_2: its photocatalytic performance, Catal. Commun. 8 (2007) 1088.
[24] M. Bagheri-Mohagheghi, N. Shahtahmasebi, M. Alinejad, The effect of the post-annealing temperature on the nano-structure and energy band gap of SnO_2 semiconducting oxide nano-particles synthesized by polymerizing–complexing sol–gel method, Phys. B: Condens. Matter 403 (2008) 2431–2437.
[25] M. Litter, Heterogeneous photocatalysis transition metal ions in photocatalytic systems, Appl. Catal. B: Environ. 23 (1999) 89–114.
[26] J. Wiszniowski, D. Robert, J. Surmacz-Gorska, K. Miksch, J.V. Weber, Photocatalytic decomposition of humic acids on TiO_2 Part I: discussion of adsorption and mechanism, J. Photochem. Photobiol. A: Chem. 152 (2001) 267–273.
[27] X. Huang, M. Leal, Q. Li, Degradation of natural organic matter by TiO_2 photocatalytic oxidation and its effect on fouling of low-pressure membranes, Water Res. 2008 (2008) 1142–1150.
[28] R.W. Matthews, Photo-oxidation of organic material in aqueous suspensions of titanium dioxide, Water Res. 20 (1986) 569–578.
[29] B. Uyguner, M. Bekbolet, A comparative study on the photocatalytic degradation of humic substances of various origins, Desalination 176 (2005) 167–176.
[30] S. Liu, M. Lim, R. Fabris, C. Chow, M. Drikas, R. Amal, Removal of humic acid using TiO_2 photocatalytic process-formation and molecular weight characterization studies, Chemosphere 72 (2008) 263–271.
[31] J.H. Park, Spectroscopic characterization of dissolved organic matter and its interactions with metals in surface waters using size exclusion chromatography, Chemosphere 77 (2009) 485–494.
[32] S.A. Huber, A. Balz, F.H. Frimmel, Identification of diffuse and point sources of dissolve organic carbon (DOC) in a small stream (Alb, Southwest Germany), using gel filtration chromatography with high-sensitivity DOC-detection, Fresenius J. Anal. Chem. 350 (1994) 496–503.
[33] F.H. Frimmel, Characterization of natural organic matter as major constituents in aquatic systems, J. Contam. Hydrol. 35 (1998) 201–216.
[34] C. Specht, M. Kumke, F.H. Frimmel, Characterization of NOM adsorption to clay minerals by size exclusion chromatography, Water Res. 34 (2000) 4063–4069.
[35] A. Piccolo, S. Nardi, G. Concheri, Micelle-like conformation of humic substances as revealed by size exclusion chromatography, Chemosphere 33 (1996) 595–602.
[36] U. Lankes, M. Müller, M. Weber, F.H. Frimmel, Reconsidering the quantitative analysis of organic carbon concentrations in size exclusion chromatography, Water Res. 43 (2009) 915–924.
[37] J. Weishaar, G. Aiken, B. Bergamaschi, M. Fram, R. Fujii, K. Mopper, Evaluation of specific ultraviolet absorbance as an indicator of the chemical composition and reactivity of dissolved organic carbon, Environ. Sci. Technol. 37 (2003) 4702–4708.
[38] P. Westerhoff, G. Aiken, G. Amy, J. Debroux, Relationships between the structure of natural organic matter and its reactivity towards molecular ozone and hydroxyl radicals, Water Res. 33 (1999) 2265–2276.
[39] C. Uyguner, M. Bekbolet, Evaluation of humic acid photocatalytic degradation by UV–vis and fluorescence spectroscopy, Catal. Today 101 (2005) 267–274.
[40] C. Uyguner, M. Bekbolet, Implementation of spectroscopic parameters for practical monitoring of natural organic matter, Desalination 176 (2005) 47–55.
[41] J. Peuravuori, K. Pihlaja, Preliminary study of lake dissolved organic matter in light of nanoscale supramolecular assembly, Environ. Sci. Technol. 38 (2004) 5958–5967.
[42] M. Kumke, C. Specht, T. Brinkmann, F.H. Frimmel, Alkaline hydrolysis of humic substances – spectroscopic and chromatographic investigations, Chemosphere 45 (2001) 1023–1031.
[43] H.C. Kim, M.J. Yu, Characterization of natural organic matter in conventional water treatment processes for selection of treatment processes focused on DBPs control, Water Res. 39 (2005) 4779–4789.
[44] S. Valencia, J. Marín, J. Velásquez, G. Restrepo, F.H. Frimmel, Study of pH effects on the evolution of properties of brown-water natural organic matter as revealed by size-exclusion chromatography during photocatalytic degradation, Water Res. 46 (2012) 1198–1206.
[45] G. Hua, D. Reckhow, Characterization of disinfection byproduct precursors based on hydrophobicity and molecular size, Environ. Sci. Technol. 41 (2007) 3309–3315.
[46] C. Murray, S. Parsons, Prelinary laboratory investigation of disinfection byproduct precursors removal using an advanced oxidation process, Water Environ. J. 20 (2006) 123–129.
[47] H. Lin, C.P. Huang, W. Li, C. Ni, S. Ismat, Y. Tseng, Size dependency of nanocrystalline TiO_2 on its optical property and photocatalytic reactivity exemplified by 2-chlorophenol, Appl. Catal. B: Environ. 68 (2006) 1–11.